

ZEUS RESULTS ON INCLUSIVE DIFFRACTION*

MARTA RUSPA

University of Eastern Piedmont, Novara and INFN Torino, Italy
e-mail: ruspa@to.infn.it

(Received January 8, 2004)

Dissociation of virtual photons, $\gamma^*p \rightarrow Xp$, has been studied in ep interactions with the ZEUS detector at HERA. The diffractive cross section, $d\sigma_{\gamma^*p}/dM_X$, is presented as a function of the photon virtuality, Q^2 . The W dependence of the diffractive and the total cross section is compared. The dependence of the diffractive structure function, $F_2^{D(3)}$, on β , the Pomeron momentum fraction probed by photon, is also studied. The data are compared to predictions based on dipole models.

PACS numbers: 01.30.Cc, 25.40.Ep, 13.60.Hb, 42.25.Fx

1. Diffraction at HERA

One of the most relevant results of the collider experiments at HERA is that a large fraction ($\sim 10\%$) of the deep inelastic (DIS) electron-proton scattering events are diffractive [1]. Such events, believed to be a soft phenomenon, can be described by Regge phenomenology, in complete analogy with hadron-hadron diffractive interactions. Within this framework, the colorless exchange mediating diffractive interactions at high energy is known as the “Pomeron” trajectory.

The discovery of diffractive events in DIS at HERA has opened the possibility of investigating the partonic nature of the Pomeron and establish a theoretical link between the Regge theory and QCD.

A schematic diagram of a diffractive DIS event is shown in Fig. 1: a photon of virtuality Q^2 coupling to the electron interacts diffractively with a proton at a center of mass energy W and squared four momentum transfer t to produce the hadronic system X with mass M_X in the final state. As a consequence of the colorless exchange the proton remains almost intact after the collision and the particle flow is suppressed in the forward direction.

* Presented at the XXXIII International Symposium on Multiparticle Dynamics, Kraków, Poland, September 5–11, 2003.

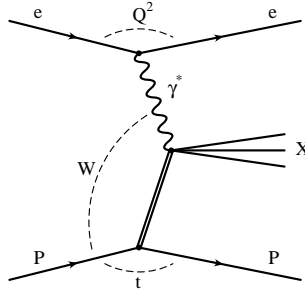


Fig. 1. Schematic diagram of inclusive diffraction in ep interactions.

2. Diffractive cross section and structure function

The cross section, $\sigma_{\gamma^*p}^D$, for the diffractive dissociation of virtual photons, $\gamma^*p \rightarrow Xp$, is related to the cross section for the process $ep \rightarrow eXp$ by

$$\frac{d\sigma_{\gamma^*p}^D}{dM_X} = \frac{\pi Q^2 W}{\alpha(1 + (1 - y)^2)} \frac{d^3\sigma_{ep}^D}{dQ^2 dW dM_X}.$$

The kinematics of the reaction $ep \rightarrow eXp$ can also be described by Q^2 in conjunction with the two dimensionless variables $x_{\mathbb{P}}$ and β , where $x_{\mathbb{P}}\beta$ is the Bjorken variable x , $x_{\mathbb{P}}$ is the fraction of the proton momentum carried by the Pomeron and β is the fraction of the proton momentum probed by the photon.

The diffractive structure function $F_2^{D(4)}$ is related to the diffractive cross section by

$$\frac{d\sigma_{ep}^D}{d\beta dQ^2 dx_{\mathbb{P}}} = \frac{4\pi\alpha^2}{\beta Q^4} \left[1 - y + \frac{y^2}{2(1 + R^{D(4)})} \right] F_2^{D(4)}(\beta, Q^2, x_{\mathbb{P}}, t),$$

where $R^{D(4)}$ is the ratio of the cross sections for longitudinally and transversely polarised photons. The diffractive structure function $F_2^{D(3)}$ is obtained by integrating $F_2^{D(4)}$ over t .

3. Results

The ZEUS collaboration presented new results [2, 3] on diffraction in DIS. Compared to the previous ZEUS analysis of this type [4–6] a higher statistics and a wider kinematic range (notably higher values of M_X up to 70 GeV, lower values of Q^2 down to 0.03 GeV² as well as values of W close to the kinematic limit) are achieved.

Diffractive events were selected by two methods: for a first data sample [2] the detection of the scattered proton in the ZEUS Leading Proton

Spectrometer was required. Although statistically limited because of the low acceptance of the LPS, this method permits the selection of events $ep \rightarrow eXp$ with negligible background from the double-dissociative reaction $ep \rightarrow eXN$, where the proton also diffractively dissociates into a state N of mass M_N that escapes undetected in the beam pipe. The LPS method also gives access to higher values of M_X (higher $x_{\mathbb{P}}$, lower β). A second data sample [3] was analysed by a method based on the characteristic of the $\ln M_X^2$ distribution, different for diffractive and non diffractive events; this method allows a higher statistics, but the sample selected is the sum of the Xp contribution and of the background contribution XN . The accessible range in hadronic mass has been substantially increased by the installation of a Forward Plug Calorimeter, which also allows to tag and reject double dissociative events with $M_N < 2.3$ GeV.

3.1. The Q^2 and W dependences of the diffractive cross section

Figure 2 shows the diffractive cross section, $d\sigma_{\gamma^*p \rightarrow Xp}^D/dM_X$, as a function of Q^2 at different M_X and W values. The present measurement is shown together with the previous ZEUS result [4] corrected for the residual double-dissociative background, taken to be 31%, as determined in [4] by comparing those data with the LPS results [5]. The data exhibit a behaviour qualitatively similar to that of the total photon-proton cross section [7]: the diffractive cross section falls rapidly with Q^2 at high Q^2 ; conversely, as $Q^2 \rightarrow 0$, the cross section dependence on Q^2 becomes very weak. The main features of the data are broadly reproduced by a fit based on the BEKW model [6,8]. This model parametrizes the diffractive cross section in terms of fluctuations of transversely and longitudinally polarised virtual photons either into $q\bar{q}$ or $q\bar{q}g$ states. In the kinematic domain of the present measurement the contribution from longitudinally polarised photons can be neglected. The β (and hence M_X) spectra of the dipole states are determined by general properties of the photon wave-function, with the $q\bar{q}$ contribution to the cross section proportional to $\beta(1 - \beta)$ and the $q\bar{q}g$ contribution proportional to $(1 - \beta)^\gamma$. The model assumes that the cross sections of the two components have a power-like behaviour in $x_{\mathbb{P}}$ of the type $(x_0/x_{\mathbb{P}})^{n(Q^2)}$, where the x_0 parameter is taken to be 0.01. In the fit, the $x_{\mathbb{P}}$ dependence was obtained from the data, along with the relative normalisation of the $q\bar{q}$ and $q\bar{q}g$ contributions and the coefficient γ . The fit was limited to the region $x_{\mathbb{P}} < 0.01$, where Pomeron exchange dominates. For small values of M_X the $q\bar{q}$ states dominate in the DIS region, while at large masses the $q\bar{q}g$ contribution becomes dominant. Going from the DIS region to the low- Q^2 region, for a given value of M_x β also decreases, and again the $q\bar{q}g$ contribution becomes dominant. The diffractive cross section, $d\sigma_{\gamma^*p \rightarrow XN}^D/dM_X$ ($M_N < 2.3$ GeV), is shown in

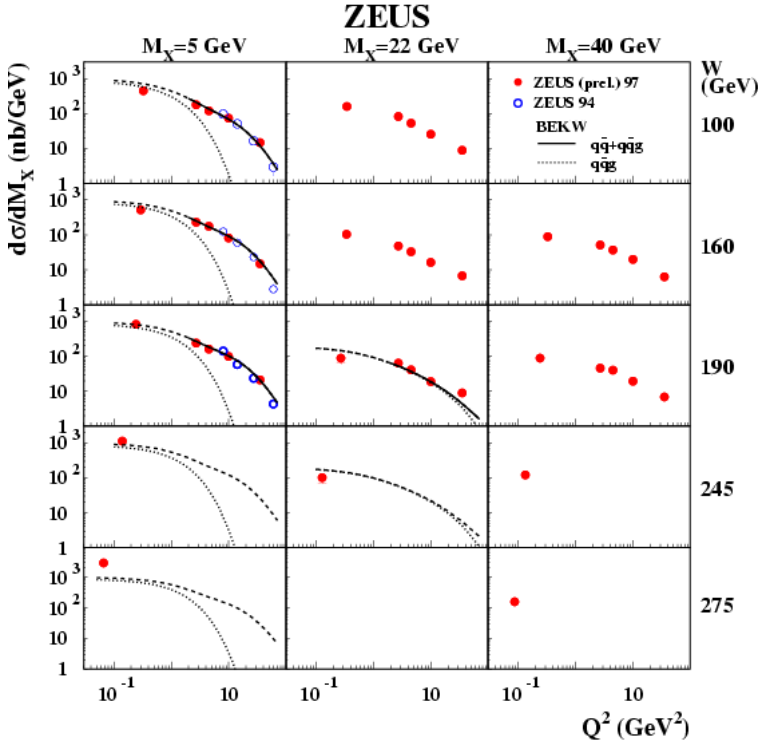


Fig. 2. The diffractive cross section, $d\sigma_{\gamma^*p \rightarrow Xp}^D/dM_X$, as a function of Q^2 at different W and M_X values. The inner error bars show the statistical uncertainties and the full bars are the statistical and the systematic uncertainties added in quadrature. The solid (dashed) lines are the results of the BEKW fit (extrapolation of the BEKW fit) described in the text. The dotted lines are the results of the same fit for the $q\bar{q}g$ contribution alone.

Fig. 3 as a function of W at different M_X and Q^2 values. For $M_X < 2$ GeV the diffractive cross section is rather constant with W . Conversely, at higher M_X , a strong rise with W is observed for all values of Q^2 . This was quantified by fitting the data for each Q^2 bin with $4 < M_X < 8$ GeV to the form

$$\frac{d\sigma_{\gamma^*p \rightarrow XN}^D}{dM_X} = h W^{a^{\text{diff}}}.$$

According to Regge models, the t -averaged Pomeron trajectory is related to a^{diff} via $\overline{\alpha}_{\mathbb{P}} = 1 + a^{\text{diff}}/4$. Measurements of hadron-hadron scattering provide $\alpha_{\mathbb{P}}^{\text{soft}} = 1.096$ [9]. Averaging over t reduces this value by about 0.02, leading to $\overline{\alpha}_{\mathbb{P}}^{\text{soft}} = 1.076$. This value is shown in Fig. 4 by the shaded

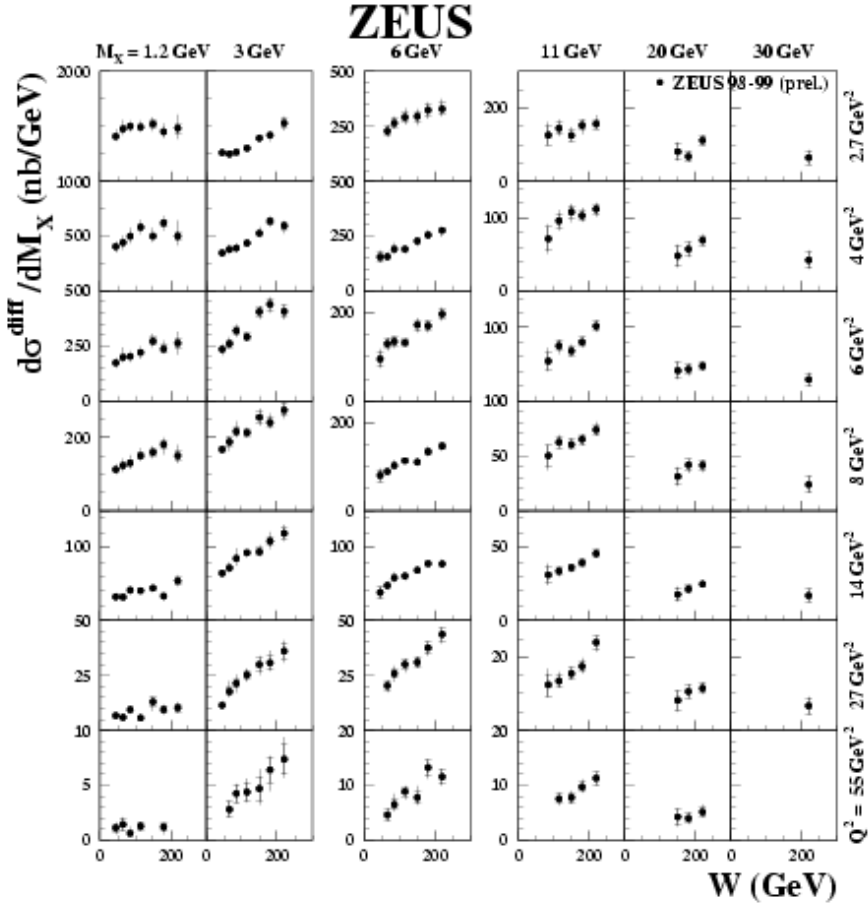


Fig. 3. The diffractive cross section, $d\sigma_{\gamma^*p \rightarrow XN}^D/dM_X$ ($M_N < 2.3$ GeV), as a function of W at different Q^2 and M_X values. The inner error bars show the statistical uncertainties and the full bars are the statistical and the systematic uncertainties added in quadrature.

band marked “soft Pomeron”. In the same figure $\alpha_{\mathbb{P}}^{\text{diff}}(0) = \overline{\alpha}_{\mathbb{P}} + 0.02$ is compared with $\alpha_{\mathbb{P}}^{\text{tot}}(0)$ obtained from the total γ^*p cross section for different Q^2 values. Both measurements are above the soft Pomeron band. The diffractive result lies approximately half-way in between the soft Pomeron and the total cross section result. In other words, the Pomeron trajectory extracted from diffraction is half as steep as that obtained from $\sigma_{\gamma^*p}^{\text{tot}}$. The diffractive data are well described by the shaded band which represents “half” of the W rise of the total cross section; therefore, for $M_X > 2$ GeV, the diffractive cross section has approximately the same W dependence of the total cross section.

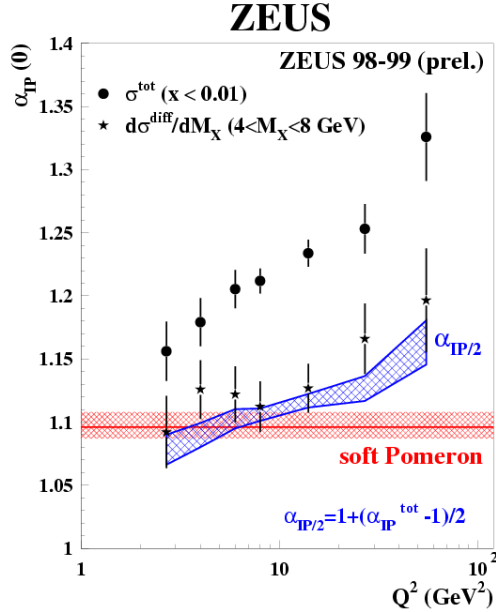


Fig. 4. The intercept of the Pomeron trajectory, $\alpha_{\mathbb{P}}(0)$, as a function of Q^2 , obtained from the W -dependence of the total γ^*p cross section and from the diffractive cross section, $d\sigma_{\gamma^*p \rightarrow XN}^D/dM_X$ ($M_N < 2.3 \text{ GeV}$), for $M_X = 4\text{--}8 \text{ GeV}$. The $\alpha_{\mathbb{P}}(0)$ values of the latter have been corrected for the t -dependence of $\alpha_{\mathbb{P}}$. The shaded band shows the expectation for a soft Pomeron. The cross hatched band represents “half” of the W -rise of the total cross section.

3.2. The β dependence of the diffractive structure function

The dependence of the diffractive structure function $F_2^{D(3)}$ on β , presented in Fig. 5 for different values of $x_{\mathbb{P}}$ and Q^2 , shows a very different behaviour at different values of $x_{\mathbb{P}}$, presumably reflecting the different partonic structure of the exchange probed. The results are compared with the prediction of the saturation model [10]. In this model [11], diffractive DIS is described as the interaction of the $q\bar{q}$ ($q\bar{q}g$) fluctuation of the virtual photon with the proton. The parameters of the $q\bar{q}$ and $q\bar{q}g$ dipole cross sections were obtained from a fit to the F_2 data. In the region of applicability of the model, $x_{\mathbb{P}} < 0.01$, the β dependence of the data is well described.

The assumption [12] that $F_2^{D(3)}$ factorises into a term which depends on the probability of finding a Pomeron carrying a fraction $x_{\mathbb{P}}$ of the proton momentum, and the structure function of the Pomeron, $F_2^{D(2)}(\beta, Q^2)$, given in terms of the quark densities of the Pomeron, leads to

$$F_2^{D(3)}(x_{\mathbb{P}}, \beta, Q^2) = f_{\mathbb{P}}(x_{\mathbb{P}}, Q^2) F_2^{D(2)}(\beta, Q^2),$$

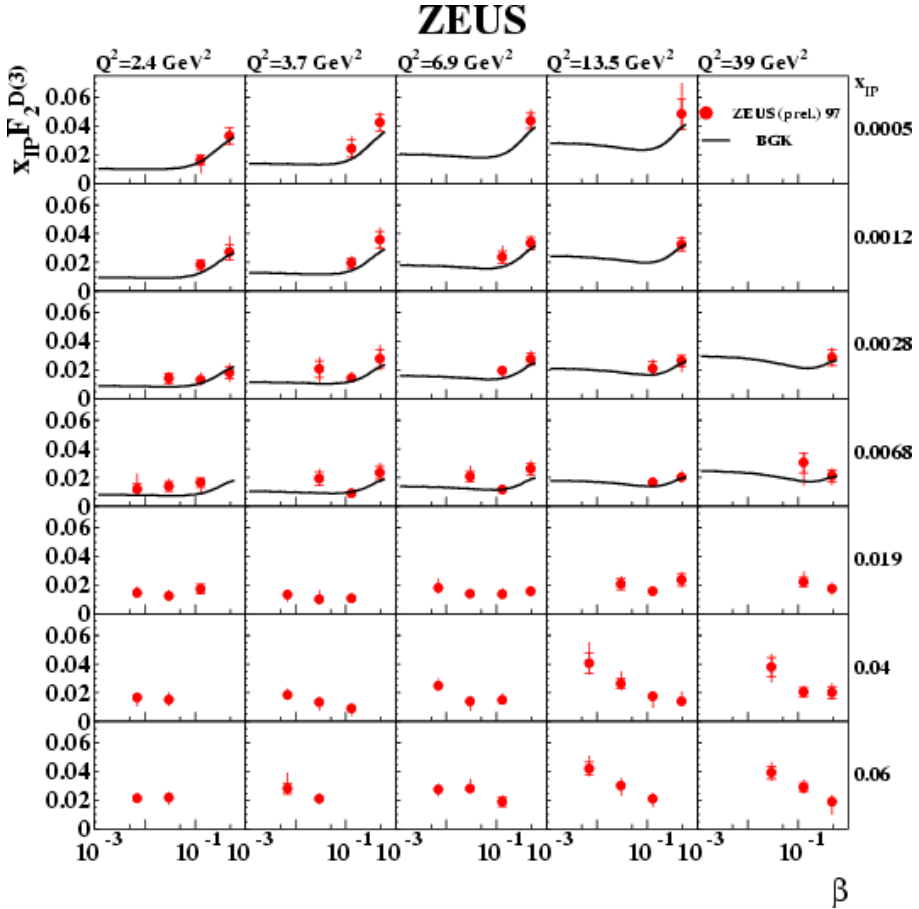


Fig. 5. The diffractive structure function multiplied by $x_{\mathbb{P}}, x_{\mathbb{P}}F_2^{D(3)}$, as a function of β , for different values of $x_{\mathbb{P}}$ and Q^2 . The inner error bars show the statistical uncertainties and the full bars are the statistical and the systematic uncertainties added in quadrature. The solid lines are the prediction of the saturation model described in the text.

with

$$f_{\mathbb{P}}(x_{\mathbb{P}}, Q^2) = \frac{C}{x_{\mathbb{P}}} \left(\frac{x_0}{x_{\mathbb{P}}} \right)^{n(Q^2)}.$$

Taking 1 for the arbitrary normalisation constants the structure function of the Pomeron can be defined as

$$F_2^{D(2)}(\beta, Q^2) = x_0 F_2^{D(3)}(x_0, \beta, Q^2).$$

In figure 6, $F_2^{D(2)}(\beta, Q^2)$ for $\gamma^*p \rightarrow XN$ ($M_N < 2.3$ GeV), as extracted near $x_{\mathbb{P}} = 0.01$, is presented as a function of β for the Q^2 values indicated. $F_2^{D(2)}$ has a maximum near $\beta = 0.5$, consistent with a $\beta(1 - \beta)$ behaviour, suggesting a main contribution from a $q\bar{q}$ state. The data indicate also that in the region of high β $F_2^{D(2)}$ decreases with increasing Q^2 . Conversely, for $\beta \rightarrow 0$, $F_2^{D(2)}$ rises with increasing Q^2 . This is reminiscent of the behaviour of the proton structure function F_2 .

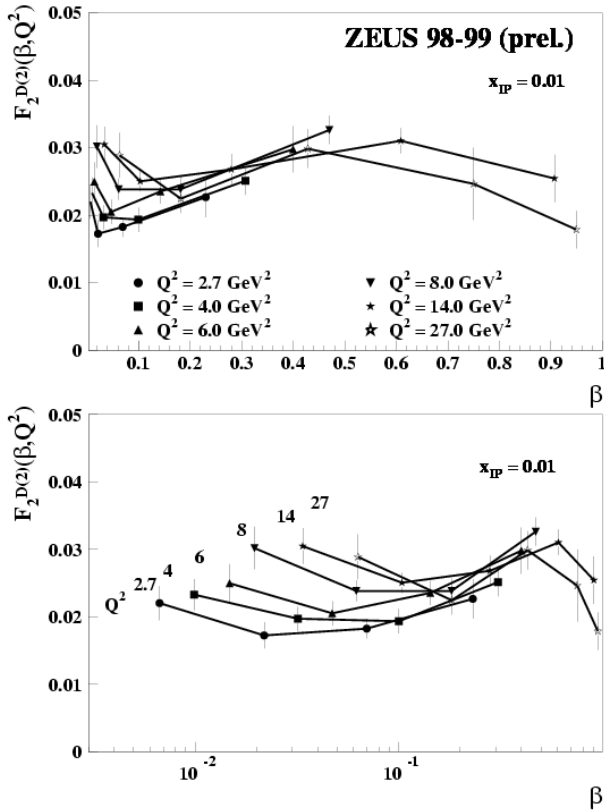


Fig. 6. The structure function $F_2^{D(2)}$ for $\gamma^*p \rightarrow XN$ ($M_N < 2.3$ GeV), as a function of β , for the Q^2 values indicated, as extracted from the $x_{\mathbb{P}}F_2^{D(3)}$ values measured near $x_{\mathbb{P}} = 0.01$. The inner error bars show the statistical uncertainties and the full bars are the statistical and the systematic uncertainties added in quadrature. The straight lines connect measurements at the same values of Q^2 .

4. Summary

A new set of ZEUS results on the diffractive DIS process $ep \rightarrow eXp$ has been presented in terms of diffractive cross sections and diffractive structure functions. The data are well described by dipole models (BEKW, saturation). The W dependences of the diffractive and of the total cross section are found to be similar at high Q^2 . From the study of the β dependence of the diffractive structure function emerges that $F_2^{D(3)}$ has a different behaviour at low and high $x_{\mathbb{P}}$; the Pomeron structure function $F_2^{D(2)}$ reveals a pQCD-like evolution with β and Q^2 .

REFERENCES

- [1] ZEUS Collaboration, M. Derrick *et al.*, *Phys. Lett.* **B315**, 481 (1993); H1 Collaboration, T. Ahmed *et al.*, *Nucl. Phys.* **B429**, 477 (1994).
- [2] ZEUS Collaboration, paper 540 submitted to EPS 2003.
- [3] ZEUS Collaboration, paper 540 submitted to EPS 2003.
- [4] ZEUS Collaboration, J. Breitweg *et al.*, *Eur. Phys. J.* **C6**, 43 (1999).
- [5] ZEUS Collaboration, J. Breitweg *et al.*, *Eur. Phys. J.* **C1**, 81 (1997).
- [6] ZEUS Collaboration, S. Chekanov *et al.*, *Eur. Phys. J.* **C25**, 169 (2002).
- [7] ZEUS Collaboration, J. Breitweg *et al.*, *Phys. Lett.* **B487**, 53 (2000).
- [8] J. Bartels *et al.*, *Eur. Phys. J.* **C7**, 443 (1999).
- [9] J.R. Cudell, K. Kang, S.K. Kim, *Phys. Lett.* **B395**, 311 (1997).
- [10] J. Bartels, K. Golec-Biernat, H. Kowalski, *Phys. Rev.* **D66**, 014001 (2002).
- [11] K. Golec-Biernat, M. Wusthoff, *Eur. Phys. J.* **C20**, 313 (2001).
- [12] G. Ingelman, P.E. Schlein, *Phys. Lett.* **B152**, 256 (1985).